Focus

Sargassum coverage in the northeastern Gulf of Mexico during 2010 from Landsat and airborne observations: Implications for the Deepwater Horizon oil spill impact assessment

Chuanmin Hu [a,*], Robert Hardy [b], Eric Ruder [c], Amelia Geggel [c], Lian Feng [a], Sean Powers [d], Frank Hernandez [e], George Graettinger [f], Jill Bodnar [f], Trent McDonald [g]

[a] College of Marine Science, University of South Florida, 140 Seventh Avenue, South, St. Petersburg, FL 33701, USA
[b] Florida Fish and Wildlife Conservation Commission, Fish and Wildlife Research Institute, 100 Eighth Avenue SE, St. Petersburg, FL 33701, USA
[c] Industrial Economics, Incorporated, 2067 Massachusetts Avenue, Cambridge, MA 02140, USA
[d] Department of Marine Sciences, University of South Alabama, 5871 USA Drive North Mobile, AL 36688, USA
[e] Department of Marine Sciences, University of Southern Mississippi, 703 East Beach Drive, Ocean Springs, MS 39564, USA
[f] NOAA Office of Response & Restoration, 7600 Sand Point Way NE, Seattle, WA 98115, USA
[g] Western EcoSystems Technology, Inc., 200 S. Second Street, Laramie, WY 82070, USA

ARTICLE INFO

ABSTRACT

Using high-resolution airborne measurements and more synoptic coverage of Landsat measurements, we estimated the total *Sargassum* coverage in the northeastern Gulf of Mexico (NE GOM) during 2010, with the ultimate purpose to infer how much *Sargassum* might have been in contact with oil from the Deepwater Horizon oil spill. Mean *Sargassum* coverage during the four quarters of 2010 for the study region was estimated to range from ~3148 ± 2355 km² during January–March to ~7584 ± 2532 km² during July–September (95% confidence intervals) while estimated *Sargassum* coverage within the integrated oil footprint ranged from 1296 ± 453 km² (for areas with >5% thick oil) to 736 ± 257 km² (for areas with >10% thick oil). Similar to previous studies on estimating *Sargassum* coverage, a direct validation of such estimates is impossible given the heterogeneity and scarcity of *Sargassum* occurrence. Nonetheless, these estimates provide preliminary information to understand relative *Sargassum* abundance in the NE GOM.

1. Introduction

Pelagic *Sargassum* macroalgae is a critical habitat for marine animals, and knowledge of its spatial distribution and temporal variability may help understand its role in modulating marine ecosystem functions, such as marine primary productivity, nutrient remineralization, bacterial activities, turtle migration, and fish abundance (Lapointe, 1995; Rooker et al., 2006; Witherington et al., 2012; Lapointe et al., 2014; Doyle and Franks, 2015). The Gulf Coast Research Laboratory of the University of Southern Mississippi has identified 139 species of fish associated with pelagic *Sargassum* (Franks et al., 2007). *Sargassum* may serve as fertilizers for sand dunes to protect shorelines, and may also be used for food, fuel, and possibly pharmaceutical materials (e.g., Milledge et al., 2015). For these reasons, the U.S. Sargasso Sea Commission and South Atlantic Fishery Management Council have identified *Sargassum* as a critical and protected marine habitat, and its harvesting in some ocean regions is regulated to protect the associated marine species (SAFMC, 2002).

Despite previous field-based studies (e.g., Huffard et al., 2014; Schell et al., 2015), our knowledge of *Sargassum*'s source and spatial/temporal variability is still limited, primarily due to lack of synoptic and frequent measurements. Such a deficiency may be overcome with remote sensing. Indeed, since the first remote sensing attempt in 2006 to detect surface pelagic *Sargassum* (Gower et al., 2006), a number of studies have tried to document *Sargassum* source, abundance, and spectral and spatial characteristics using satellite and airborne measurements (Gower and King, 2011; Gower et al., 2013; Dierssen et al., 2015; Hu et al., 2015). However, remote sensing often suffers from inadequate spatial resolution and temporal coverage due to cloud cover and other factors (Hu et al., 2015). For example, the distribution statistics based on observations from the Medium Resolution Imaging Spectrometer (MERIS, 1.2-km resolution) has shown considerable amounts of *Sargassum* in the western Gulf of Mexico (GOM) but almost none in the eastern GOM (Gower and King, 2011), likely due to the coarse resolution of MERIS, as it cannot detect small *Sargassum* patches (e.g., <~5 m in width regardless of the raft length, Hu et al., 2015). As a result, we

have very little understanding of *Sargassum* abundance in the eastern GOM.

Understanding the extent and abundance of *Sargassum* is important when trying to determine *Sargassum* exposure to surface oil during the 2010 Deepwater Horizon (DWH) oil spill (Camilli et al., 2010, McNutt et al., 2011) in the NE GOM. With an estimated volume of 3.19 million barrels of crude oil and an unknown amount of gas released over 84 days (22 April–15 July 2010; U.S. v. BP et al., 2015), DHW is the largest offshore spill in the U.S. history, yet understanding its potential impact to the marine environment has presented a significant challenge to the research community. One such challenge has been estimation of *Sargassum* abundance in the spill region, as *Sargassum* may be harmed after being in contact with oil (Powers et al., 2013).

During and after the DWH oil spill, several efforts to map the surface oil content and *Sargassum* abundance in the NE GOM were conducted. These include AVIRIS airborne hyperspectral measurements during the DWH spill (Sun et al., 2016), surface oil footprint and oil volume through synthetic aperture radar (SAR) and other satellite observations (Hu et al., 2011; Garcia-Pineda et al., 2013; Graettinger et al., 2015; MacDonald et al., 2015), targeted *Sargassum* studies involving aerial photography and aerial line transects in 2010 and 2011 (during and post- DWH spill) (Powers et al., 2013; McDonald and Powers, 2015), and Landsat remote sensing data collected in 2010 and 2011. Due to the limited number of airborne *Sargassum* AVIRIS surveys, these data could not be used to generate statistics on monthly and seasonal scales. Landsat data (30-m resolution), however, may provide a compromise between resolution and coverage for generating such statistics, as both Landsat-5 and Landsat-7 can provide repeated measurements every 16 days. Therefore, with all these available data and the pressing need to assess *Sargassum* abundance in the NE GOM during 2010, this study was undertaken to achieve the following three objectives:

1) Determine uncertainties in the Landsat-based estimates of *Sargassum* abundance
2) Develop a practical method to account for such uncertainties
3) Provide estimates of *Sargassum* abundance in the study region for different seasons.

2. Data and methods

This study involved the analyses of several data sources, including Landsat (from the USGS), AVIRIS (from NASA JPL), and low-altitude aerial digital photography (from NOAA, as part of the DWH NRDA in 2010–2011, and from National Science Foundation and GOM Research Initiative-funded surveys in 2010 and 2011, respectively). The characteristics of these different data sources are listed in Table 1. The higher-resolution sensors (i.e., AVIRIS or aerial photography) have fewer days of coverage.

2.1. Landsat

Landsat data collected during 2010 and 2011 within the northern GOM were processed and examined for the presence and coverage of *Sargassum* (Fig. 1a). In Fig. 1a, each square (or "granule") represents a Landsat scene coverage, denoted by its path and row (e.g., p18r39). Landsat paths 18 to 21 and rows 39 to 41 were considered as they cover the cumulative oil spill footprint (Graettinger et al., 2015;

MacDonald et al., 2015). The Landsat scenes annotated with an "O" in Fig. 1a are available primarily between May and August 2010 (as a response by the USGS to the DWH oil spill), with only three exceptions: one scene in January 2010 for p18r41, p19r40, p19r41, p20r40, and p20r41; two scenes in February 2010 for p21r41; and several scenes in December 2010 for p18r41 and p21r41. Table 2 lists the number of Landsat scenes used to derive *Sargassum* coverage statistics during each quarter of 2010 for each Landsat path. Note that the 2011 Landsat scenes were used to derive a calibration equation with airborne photos, and therefore are not listed in Table 2.

Landsat data were corrected to remove the atmospheric gas absorbing and scattering effects, and then converted to Rayleigh-corrected reflectance (R_{rc}, dimensionless). The data were used to compose two types of images: Red-Green-Blue (RGB) true color composites and Floating Algae Index (Hu, 2009). Following Hu (2009), FAI was derived as:

$$FAI = R_{rc,NIR} - R_{rc,red} - (R_{rc,SWIR} - R_{rc,red})(\lambda_{NIR} - \lambda_{red})/(\lambda_{SWIR} - \lambda_{red}), \quad (1)$$

where the subscripts NIR, red, and SWIR represent the spectral bands. For Landsat, $\lambda_{NIR} = 660$ nm, $\lambda_{RED} = 825$ nm, $\lambda_{SWIR} = 1650$ nm.

Between late April 2010 and mid July 2010, emulsified oil slicks on the ocean surface could be visualized from the Landsat RGB and MODIS images (Hu, 2009; Hu et al., 2011) because these slicks show enhanced reflectance in the red and near-infrared wavelengths. It was difficult to differentiate them from *Sargassum* slicks using Landsat data alone. Therefore, to avoid counting these pixels as *Sargassum*, the ambiguous slicks within the oil spill footprint (delineated from individual Landsat images) were discarded from the analysis. They were treated in the same manner as clouds or no coverage, and were not used in the calculation of the fractional *Sargassum* coverage below. Note that although *Sargassum* in the ocean may form surface mats and weedlines of various shapes, in this context from the perspective of detection from remote sensing imagery they are termed as *Sargassum* slicks.

The RGB and FAI images were examined together to identify potential *Sargassum* slicks. The former was used to visualize clouds, water, surface oil, and other features, while the latter examined the NIR feature to detect floating *Sargassum* (with the aid of visual interpretation and spectral analysis). Fig. S1 in Supplemental materials shows that FAI is nearly immune to thin clouds, and the distinguished slick feature is associated with R_{rc} spectra representing floating vegetation. Such outstanding slick features were manually delineated on each image. Each pixel of the image was classified as algae, algae-free water, or no-observation (clouds or land). For each Landsat scene, the *Sargassum* percent coverage was calculated as *Sargassum* area divided by searched area as:

$$P_{a,Lansat} = \#of\ algae\ pixels/$$
$$(\#of\ algae\ pixels + \#of\ algae-free\ water\ pixels) \times 100\%.$$
$$(2)$$

The size of the water area covered by the Landsat paths was calculated within ArcGIS with overlapping edges considered as separate paths (Table 3). The overlapping portions of Landsat paths were considered separately (Table 3; Fig. 1a). Also, any instances of overlap within rows were averaged to avoid double counting. The resulting percent coverage values were multiplied by the area covered by Landsat paths. Regions of

Table 1
Satellite and aerial photographic data used in this study.

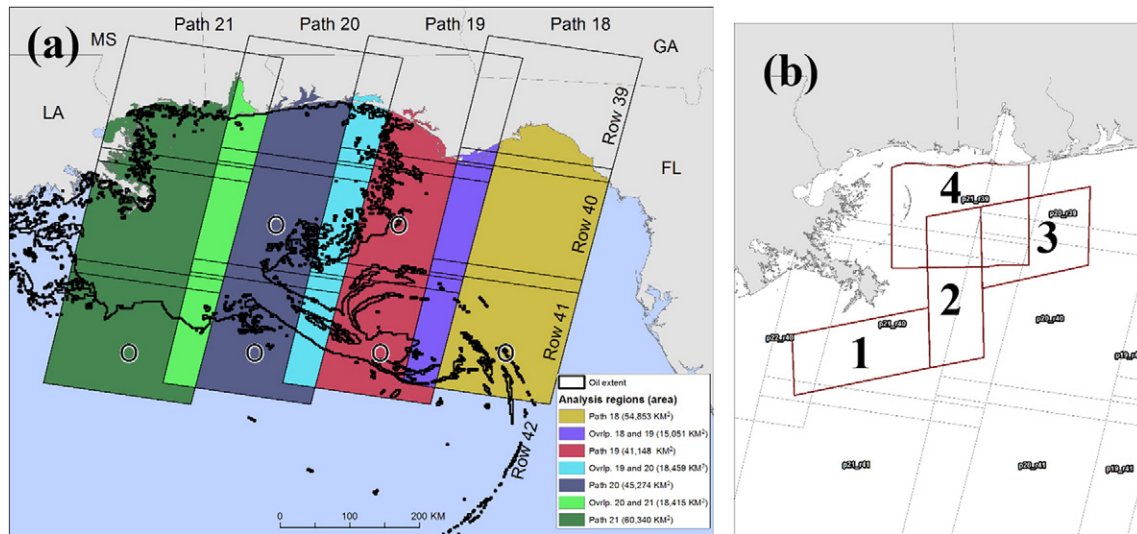| Sensor	Spatial resolution	Swath	Spectral resolution	Revisit
Landsat5 TM	30 m	180 km	Multi-band, 450 to 1640 nm	16 days
Landsat7 EMT +	30 m	180 km	Multi-band, 450 to 1640 nm	16 days
AVIRIS	8 to 15 m	20 to 40 km	Hyperspectral, 350 to 2100 nm	Event response
Aerial photography	30 to 40 cm	<1 km	Red–green–blue photo	Event response

Fig. 1. (a) Availability and area of northern GOM Landsat scenes from paths 18–21, rows 39–41. The scenes marked with an "O" are available primarily between May and August 2010 (as a response by the USGS to the DWH oil spill), with only three exceptions: one scene in January 2010 for each of p18r41, p19r40, p19r41, p20r40, p20r41; two scenes in February 2010 for p21r41; several scenes in December 2010 for p18r41 and p21r41. Note that the overlap between two adjacent paths is defined separately in this study to avoid double counting. (b). Four areas (red outlines) were measured for *Sargassum* areal and fractional coverage using targeted airborne surveys during 2011: 1. Venice; 2. Mobile; 3. Pensacola; 4: NSF/GoMRI.

overlap were assigned the average coverage of the two adjacent regions. The extent of oiling was obtained by intersecting the integrated MODIS oil footprint (Graettinger et al., 2015) with the Landsat path summary regions (Fig. 1a, Table 3).

For each Landsat granule in Fig. 1a, most months have more than two scenes because data were available from both Landsat-5 TM and Landst-7 EMT+. The total number of scenes examined and the number of scenes in which *Sargassum* was observed are presented in Table 2. During statistical analysis, all examined Landsat scenes were considered, regardless of the presence or absence of *Sargassum*. The only month and path combination with no data was Path 18 in March 2010, so the seasonal summary for Path 18 and Jan.-Mar. 2010 used data only from January and February 2010.

2.2. AVIRIS

A total of 456 AVIRIS flight lines were collected between 6 May and 22 July 2010, and geo-referenced and calibrated radiance data (L_t, mW cm^{-2} µm^{-1} sr^{-1}) were obtained from NASA JPL for each flight line. An initial attempt to convert the L_t data to atmospherically corrected surface reflectance (R, dimensionless) was through the software module ATREM. However, spectral analysis of R showed frequent negative reflectance in the blue bands and very noisy results in some of the NIR bands due to uncertainties in correcting the absorbing gases and aerosols. Due to these factors, the analysis used the AVIRIS total radiance (L_t) data only. It was found that floating algae had unique spectral shape from other surface features (including weathered oil). Namely, there is a local L_t minimum around 670 nm due to pigment absorption, accompanied with elevated L_t in the NIR due to the red-edge reflectance of floating

algae (Fig. S2). These features were used to delineate *Sargassum* in AVIRIS imagery collected on the same day as Landsat.

2.3. Airborne photography

Digital photos from low-altitude flights taken during the DWH response, available from NOAA Natural Resource Damage Assessment (NRDA), were collected and analyzed for the presence/absence of *Sargassum*. Each photo had the attributes of date/time and location (latitude and longitude), thus could be visually compared with concurrent AVIRIS measurements to determine the uncertainties in AVIRIS measurements.

2.4. Airborne coverage estimates from line transects

Two studies flew randomly chosen aerial line transects in 4 blocks roughly covering the Landsat-surveyed area (Fig. 1b). These were from targeted projects funded by the National Science Foundation and GoM Research Initiative. Transects in blocks 1, 2, and 3 were flown by helicopter during 2010 and 2011, while transects in block 4 were flown using a fixed-wing aircraft during the same time period (Table 4). During aerial surveys, crews visually identified *Sargassum* mats, lines, and scattered clumps and measured distance off transect to the sighted target. Surface based crews subsequently measured the sizes of mats and lines by either circumnavigation or transit though the lines. Aerial crews measured the sizes of scattered clumps by recording start and stop coordinates when entering scattered clump fields. Using distance sampling methods (Buckland et al., 2001), McDonald and Powers (2015) estimated density of each target type (mats, lines, and scattered clumps), and multiplied by average target size to arrive at an estimate of total extent of *Sargassum*, from which the *Sargassum* proportion of the survey area was calculated as $P_{a,air}$.

Table 2

Number of scenes examined and those containing *Sargassum* (in parenthesis) per Landsat path for Landsat rows 39–41 during 2010. The 2011 Landsat scenes were used to derive a calibration equation with airborne photos, and therefore not listed here.

Season	Path 21	Path 20	Path 19	Path 18
Jan–Mar	14 (4)	6 (1)	6 (0)	6 (1)
Apr–Jun	17 (10)	6 (6)	7 (3)	8 (5)
Jul–Sep	23 (13)	16 (11)	12 (11)	16 (14)
Oct–Dec	17 (7)	5 (2)	5 (0)	13 (5)

Table 3

Water and oil area of Landsat path analysis regions in Fig. 1a (rows 39–41). Note that the overlapping regions between adjacent paths were considered separately to avoid double counting.

	P 21	P 21 & 20	P 20	P 20 & 19	P 19	P 19 & 18	P 18
Area (km^2)	60,340	18,415	45,274	18,495	41,148	15,051	54,853
Oil area (km^2)	34,138	13,665	28,169	10,404	10,591	423	1083

Table 4
Dates of airborne surveys in NE GOM.

Survey Area	Size	Number of surveys	Dates surveyed
Venice	2000 square nautical miles	16	03-Dec-2010, 14-May-2011, 20-May-2011, 26-May-2011, 06-Jun-2011, 11-Jun-2011, 19-Jun-2011, 27-Jun-2011, 17-Jul-2011, 23-Jul-2011, 25-Jul-2011, 21-Aug-2011, 28-Aug-2011, 12-Sep-2011, 15-Sep-2011, and 20-Sep-2011
Mobile	2000 square nautical miles	7	09-May-2011, 07-Jun-2011, 07-Jul-2011, 18-Jul-2011, 03-Aug-2011, 16-Aug-2011, and 11-Sep-2011
Pensacola	2000 square nautical miles	10	09-Nov-2010, 12-Nov-2010, 17-May-2011, 23-May-2011, 16-Jun-2011, 23-Jun-2011, 13-Jul-2011, 21-Jul-2011, 16-Sep-2011, and 24-Sep-2011
NSF	3365 square nautical miles	5	16-Jun-2010, 14-Jul-2010, 21-Jul-2010, 18-Aug-2010, 08-Sep-2010
GoMRI	3365 square nautical miles	6	22-Jul-2011, 26-Jul-2011, 17-Aug-2011, 09-Sep-2011, 15-Sep-2011, 21-Sep-2011, and 28-Sep-2011

2.5. Cross-sensor comparison and calibration

An extensive effort was made to find concurrent (same day or from adjacent days) data collected by two of the sensors over the same locations. Once a concurrent pair of images was found, the *Sargassum* coverage was first visually inspected, and then a relationship between the areal coverage or *Sargassum* proportion (P_A) of the two observations was attempted. Once a statistically meaningful calibration relationship was established, it was applied to one of the observations (in this case, Landsat) to scale up the other observation (airborne line transects).

2.6. Surface oil footprint

To estimate the area and extent of surface oil to which *Sargassum* was exposed, an intensive analysis of daily surface oil coverage based on multiple satellite sensors from April to August 2010 was conducted (Graettinger et al., 2015). Two sets of cumulative oiling footprints have been developed, based on two levels of percent cover of surface oil and two time periods. The surface oiling data set provides information on the area of the ocean where there was oil with a given percent being covered by "thick oil." These polygons include ocean area that had surface oiling for at least one day. Based on expert opinion informed by field observation of both surface oil and *Sargassum*, two cutoffs of the percent area covered by thick oil were selected to bound the likely exposure of *Sargassum* to oil: areas with >5% thick oil and areas with >10% thick oil.

3. Results

Due to the huge data volume, a complete list of images analyzed in this effort cannot be presented. Some sample images from Landsat, AVIRIS, and aerial photography are provided in Supplemental materials (Figs. S1–S3) to demonstrate how *Sargassum* was interpreted from each type of imagery.

Of a total of 177 Landsat scenes with minimal cloud cover in 2010, 93 were found to contain *Sargassum* slicks of variable amounts (Table 2), indicating that the odds of observing *Sargassum* was >50%. However, when trying to compare with concurrent AVIRIS or airborne photos, significant mismatches were found due to their different resolutions.

3.1. Landsat – AVIRIS comparison

Despite the 456 AVIRIS flight lines and 177 Landsat scenes examined in this study, only two AVIRIS flight lines on 24 May 2010 (Run05 and Run06) were found to have collocated and concurrent measurements with Landsat. Based on statistics of these two AVIRIS lines with concurrent Landsat *Sargassum* maps, Landsat estimates of *Sargassum* area coverage (without weighting the pixels) agrees with AVIRIS to within ±30% (Hu et al., 2015). While Landsat pixels (30-m) are larger than AVIRIS pixels (8–15 m depending on flight altitude) and Landsat may overestimate the area coverage for the identified pixels, Landsat may miss some small *Sargassum* patches for the same reason. These two

factors offset each other, leading to the observed difference. In other words, from the limited comparison, AVIRIS-derived *Sargassum* coverage estimates are similar in magnitude to Landsat-derived coverage estimates.

3.2. AVIRIS — airborne photo comparison

AVIRIS pixels are not small (~8 m per pixel), and they may also miss relatively small *Sargassum* patches. Indeed, concurrent aerial photography and AVIRIS measurements suggested that AVIRIS ground resolution (8 to15 m) was not sufficient to capture small *Sargassum* patches. Concurrent AVIRIS/aerial photograph pairs were found only during three days in 2010 (5/18/2010, 5/24/2010, and 7/12/2010). Of these cases, only aerial photographs taken on 5/24/2010 (5 of the 24) showed *Sargassum* mats, and these mats were completely missed by concurrent AVIRIS images. It was also impossible to determine statistically how much *Sargassum* AVIRIS might have missed due to the small sampling size because only three days were available.

3.3. Landsat — airborne photo comparison

Because Landsat resolution is coarser than AVIRIS, it was speculated that Landsat may miss small *Sargassum* patches. From the entire data archived, eight cases of concurrent Landsat and airborne observations were found, three of which were in 2010 (7/21/2010, 11/9/2010, and 12/3/2010) while the other five were in 2011 (7/7/2011, 7/23/2011, 8/16/2011, 9/17/2011, and 9/25/2011). The results show that the aerial photography-identified *Sargassum* mats were nearly completely missed by concurrent Landsat observations (Hu et al., 2015).

3.4. Scaling Landsat observations using Landsat/airborne line transect calibration equation

The limited concurrent and collocated data make it impossible to directly relate Landsat-derived *Sargassum* coverage to that derived from low-altitude aerial observations based on regression between the features. Alternative ways must be used to scale Landsat observations using aerial observations, if the latter are regarded to be close to the truth. In this study, after many trial and errors, a scaling factor was derived to account for the missing *Sargassum* mats by Landsat observations in the following way.

Specifically, observations from Landsat and airborne line transects (Table 4) on "concurrent" days during 2011 were used to scale Landsat *Sargassum* coverage. In order to maximize the number of image pairs, data collected within ±3 days were considered as concurrent. We initially limited the Landsat-aerial photography pairs to days when wind speed (obtained from NCEP) was <5 m s^{-1} between the two observations. Because only nine pairs met this criteria, we considered all 27 pairs that overlapped within ±3 days, regardless of windspeed in order to make the regression statistically meaningful. The 27 data pairs were used to derive a scaling relationship, as shown in

Fig. 2 and Eq. (3).

$$
\begin{aligned}
E[\text{airborne line transect}] \\
= (0.066060 + 0.004935 \log(x+c)) \pm 2.0595 \\
\times \sqrt{0.01106991^2 \left[\frac{1}{27} + \frac{(\log(x+c) + 10.85271)^2}{64.96884} \right]}
\end{aligned}
\tag{3}
$$

where $c = 7.57\,E^{-6}$ and log was the natural logarithm. The terms after "$\pm$" represent 95% confidence intervals. These equations were used to calibrate a Landsat coverage value of x to a corresponding airborne-observed coverage E. For example, if the Landsat coverage proportion on a particular day in a particular region was $x = 0.0008$, the coverage proportion based on airborne line transect would be predicted to average $0.066060 + 0.004935\log(0.0008 + c) = 0.030914 = 3.1\%$. Note that for a Landsat coverage of 0.0, the corresponding airborne-observed coverage is 0.0079 ($=0.79\%$) (offset on the y-axis of Fig. 2).

The calibration equations were applied to each Landsat scene in Table 2. Correspondingly, the Sargassum coverage proportion determined by Landsat for each scene was scaled based on the calibration equations provided in Fig. 2 and Eq. (3). All scenes within each path or overlapped path (Fig. 1a, Table 3) during each quarter were considered together to calculate a mean coverage proportion, P_{mean}, which was then multiplied by the water area in Table 3 to result in the estimated Sargassum area coverage (in km²). Integration of the coverage over all paths or over the oil footprint resulted in the total Sargassum coverage.

Detailed results for each path, together with their individual coverage proportion, can be found in Tables S1 and S2 in the Supplemental materials. Fig. 3 and Table 5 provide a summary of the seasonal coverage (with 95% confidence intervals) for each quarter in 2010. The summary was generated using Eq. (2) and Landsat data as follows.

Fig. 3. Mean Sargassum aerial coverage during each quarter of 2010 for waters covered by Landsat path 18–21 row 39–41. The vertical bars represent the 95% confidence intervals.

For each season, integrated Sargassum coverage (over all paths) was computed as

$$
E[\text{season total}] = \sum_{i \in Paths} a_i E_i[\text{airborne}],
\tag{4}
$$

where $a_i = $ area of the ith path (km²). Confidence limits on seasonal coverage were computed by

$$
CI[\text{season total}] = E[\text{season total}] \pm 1.96\,se[\text{season total}]
\tag{5}
$$

where

$$
se[\text{season total}] = \sqrt{\sum_{i \in Paths} a_i^2 (se_i[\text{airborne}])^2},
\tag{6}
$$

and

$$
se_i[\text{airborne}] = \sqrt{0.01106991^2 \left[1 + \frac{1}{27} + \frac{(\log(x+c) + 10.58271)^2}{64.96884} \right]}
$$

was the estimate of standard error for percent coverage in the ith path. Note that seasonal summaries apply to larger areas than single paths, and that precision of seasonal totals is generally higher than precision of path values. For example, lower confidence limits in Appendix I may be 0 across all paths, but the lower confidence limit can be >0 on the seasonal total because it is summarized over bigger area.

Fig. 3 shows the results scaled to the entire path area. These results show a clear seasonality, where the months of April to September showed substantially higher Sargassum coverage than the months of October to March.

4. Discussion

4.1. Uncertainties

Estimating Sargassum coverage is technically challenging, primarily due to inadequate spatial resolution and spatial/temporal coverage, as seen in cross-comparisons between Landsat (30-m) and AVIRIS
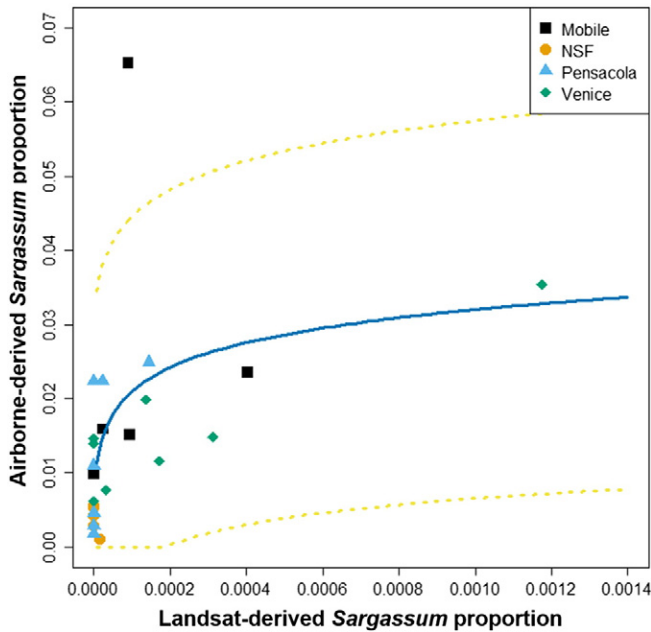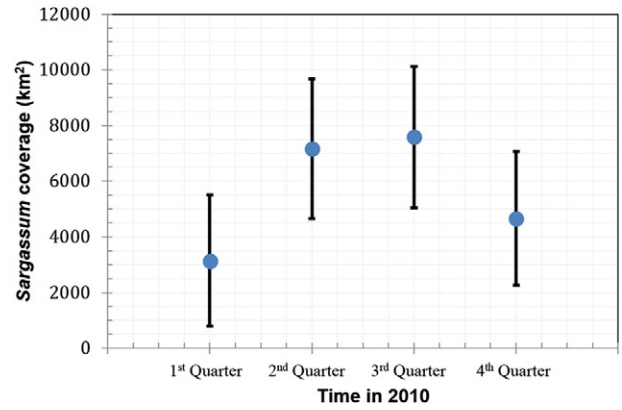

Fig. 2. Relationship between Landsat derived Sargassum coverage proportion (Eq. (2)) and aerial line-transect derived Sargassum coverage proportion, without wind restriction. This relationship was used to calibrate Landsat-derived estimates. Yellow dashed lines outline 95% confidence intervals for mean aerial coverage estimates at fixed levels of Landsat estimates. The fitting equations for the solid line and dashed lines are provided in Eqs. (3) and (4). The color legend represents the airborne survey regions denoted in Fig. 1b. Figure reproduced from McDonald (2015).

Table 5
Seasonal total Sargassum coverage estimates and standard errors computed by Eqs. (4) and (6).

Quarter in 2010	Seasonal total coverage (km²; Eq. (4))	Standard error, seasonal total (Eq. (6))
Jan–Mar	3148.41	1201.737
Apr–Jun	7170.82	1278.975
Jul–Sep	7584.00	1291.950
Oct–Dec	4667.94	1222.275

(8–15 m), between AVIRIS and low-altitude aerial photography (30–40 cm), and between Landsat and low-altitude aerial line transects. Prior studies of *Sargassum* using MERIS data (300-m and 1.2-km resolutions) did not detect *Sargassum* in the NE GOM for any time of the year (Gower and King, 2011). In this study, both Landsat and AVIRIS showed *Sargassum* slicks of variable amounts. However, nearly all *Sargassum* patches caught on low-altitude aerial photography or aerial line transects were missed by Landsat or AVIRIS.

Given the common knowledge that *Sargassum* can be very scattered and most patches are small (meters or sub-meters), such a finding is not surprising. However, the question then becomes how can we estimate how much *Sargassum* Landsat may have missed. Without complete coverage of sub-meter resolution imagery, this question is impossible to address directly. The proposed scaling method (Eq. (3)) may then be the only feasible approach to address this question indirectly, with the assumption that the *Sargassum* percent coverage is the same between concurrent and collocated Landsat and aerial observations from the line transects.

Clearly, such an approach must have large uncertainties, especially when considering that "concurrent" in this study was defined as ±3 days in order to have enough pairs to perform statistical analysis. Another source of potential uncertainty is that the consecutive Landsat paths were covered on different days. Some of the *Sargassum* mats may have been advected from one path to another, causing possible overestimation in one path and underestimation in another. Whether these two factors cancel each other is unknown.

Furthermore, the entire estimates were based the calibration equation from visual interpretations of low-altitude airborne line transects (McDonald and Powers, 2015). The subjectivity of visual inspection represents another source of uncertainty. However, the aerial surveys used in developing the calibration equations were objectively designed to take transect lines in pre-defined grids with calibrations from concurrent shipborne measurements of *Sargassum* size. This design likely removes the user bias of targeting only suspicious features. In any case, the results or the scaling equations used here should not be extended to other regions or other years, as the current approach was specifically designed for a specific time in a restricted region.

4.2. Implications for impact assessment of the DWH oil spill

The estimates in Fig. 3 provide integrated mean *Sargassum* coverage for the Landsat paths. It is unknown whether during the months of late April to late July (95 days in total) all these *Sargassum* patches were in contact with the surface oil, as the results did not contain information on exactly when and where the *Sargassum* slicks were found. However, with the surface oil footprints (5% thick and 10% thick) obtained from multiple satellites (Doiron et al., 2014, Fig. 4), the following may provide a crude estimate.

Sargassum moves across the N GOM with currents and winds, taking approximately six weeks to move across the full range of the area affected by the spill. As a result, all the *Sargassum* in the area affected by oil is replaced after six weeks. Accordingly, exposure of *Sargassum* to surface oil was assessed in two separate six-week time frames: the early part of the spill (April 25 to June 5, 2010) and the latter part of the spill (June 6 to July 17, 2010). *Sargassum* present at the beginning of the spill was assumed to be oiled and injured as it moved through the spill area for six weeks and then replaced by additional *Sargassum* over the following six weeks. The total amount of *Sargassum* injured by the spill is the sum of quantities in areas of thick oil for these two time periods.

The *Sargassum* coverage within the 5% and 10% thick-oil footprints in Fig. 4 was estimated through multiplying the percentage coverage by the oil footprint size, with upper- and lower-bound 95% intervals also estimated. The results are listed in Table 6. The total amount of oiled *Sargassum* ranges from 843 to 1749 km² within areas where the surface was covered by >5% thick oil. This includes 479 to 993 km² within areas where coverage was >10% thick oil. Note that these estimates are based on several assumptions due to limited data coverage, therefore carrying similar uncertainties as when airborne observations were used to scale up Landsat observations. Nevertheless, the ±95% confidence intervals may provide lower and upper bounds of these estimates.

4.3. Implications for future event response effort

Two lessons have been learned from this effort for event response and for post-event assessment, respectively. First, the effort suffered from lack of field data during the spill. Although low-altitude airborne photos were taken during the spill, these images were taken in a subjective way (i.e., a photo was taken if a certain feature was sighted visually). In addition, field measurements of *Sargassum* (reflectance spectra, biomass, etc.) were not taken. Targeted and objective measurements need to be implemented for future event response, for example by deploying hyperspectral airborne instruments specifically for *Sargassum* mapping (e.g., Marmorino et al., 2011; Dierssen et al., 2015) but with high-resolution flight lines objectively designed for mapping purpose (similar to the line transect-interpreted data used here to scale Landsat observation), or by field measurements through net towing (Schell et al., 2015). Indeed, *Sargassum* can be very patchy in the ocean when they form mats, lines, and scattered clumps, and even low-resolution airborne sensors (e.g., 8–15 m resolution of AVIRIS) can miss those small patches (Hu et al., 2015). High-resolution sensors or ship-based net tows are necessary to accurately estimate the *Sargassum* abundance. Second, relevant to the post-event assessment, an enormous amount of effort was dedicated to design and implement the strategy for *Sargassum*
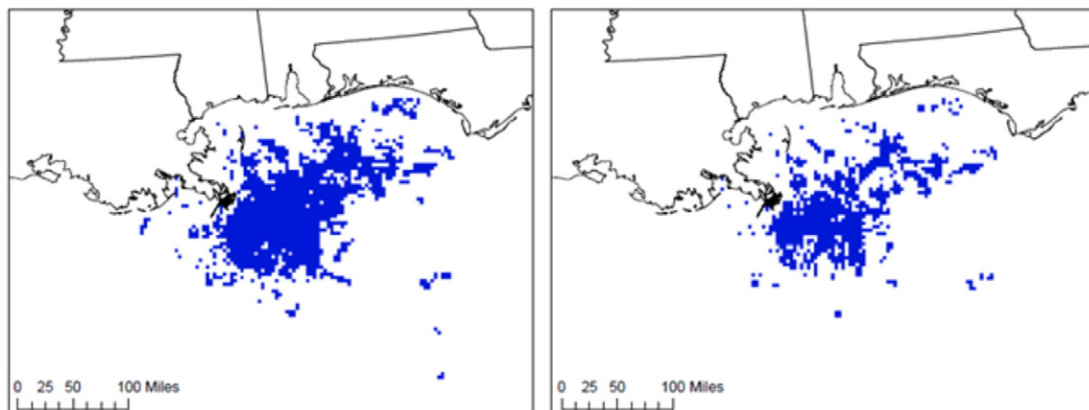

Fig. 4. Cumulative areas of surface oiling displaying the total area in the NE GOM with at least one day of >5% thick oil (45,825 km²; left) and >10% thick oil (26,025 km²; right). Figure from Doiron et al. (2014).

Table 6
Area of *Sargassum* within oiling footprint (km²).

% thick oil	Lower bound	Central estimate	Upper bound
>5%	843	1296	1749
>10%	479	736	993

mapping, and these tasks and activities have undergone several rounds of revisions. Substantial efforts from several partnering groups have been carried out to revise, refine, implement, and execute the various tasks. Such experience will serve as invaluable reference when assessing potential damage in the event of another spill.

5. Conclusion

The most significant result from this study is the finding that all satellite instruments and high-altitude airborne instruments will miss significant amounts of *Sargassum* in all seasons. Therefore, even though they could provide general distributions of large *Sargassum* patches, satellite data alone are insufficient to provide accurate estimates of the total *Sargassum* coverage. Scaling factors using the much higher-resolution observations from low-altitude airborne measurements are required to provide a more accurate estimate of *Sargassum* coverage. At present, the Landsat-based *Sargassum* coverage estimates scaled using low-altitude airborne measurements represent our best knowledge of *Sargassum* coverage before, during, and after the DWH oil spill in 2010.

Acknowledgment

Appendix A. Supplementary data

Supplementary data to this article can be found online at http://dx.doi.org/10.1016/j.marpolbul.2016.04.045.

References

Buckland, S.T., Anderson, D.R., Burnham, K.P., Laake, J.L., 2001. Introduction to Distance Sampling: Estimating Abundance of Biological Populations. Oxford University Press.

Camilli, R., Reddy, C.M., Yoerger, D.R., Van Mooy, B.A., Jakuba, M.V., Kinsey, J.C., McIntyre, C.P., Sylva, S.P., Maloney, J.V., 2010. Tracking hydrocarbon plume transport and biodegradation at Deepwater Horizon. Science 330, 201–204.

Dierssen, H., Chlus, A., Russell, B., 2015. Hyperspectral discrimination of floating mats of seagrass wrack and the macroalgae *Sargassum* in coastal waters of Greater Florida Bay using airborne remote sensing. Remote Sens. Environ. http://dx.doi.org/10.1016/j.rse.2015.1001.1027.

Doiron, K., Geggel, A., Ruder, E., 2014. Oil on water time series analysis methods for assessment of injury to *Sargassum* and *Sargassum*-dependent fauna. (WC_TR.26). DWH Water Column NRDA Technical Working Group Report.

Doyle, E., Franks, J., 2015. *Sargassum* Fact Sheet. Gulf and Caribbean Fisheries Institute (4 pp.).

Franks, J., Hoffmayer, E., Comyns, B., Hendon, J., Blake, E., Gibson, D., 2007. Investigations of fishes that utilize pelagic *Sargassum* and frontal zone habitats in Mississippi marine waters and the northern Gulf of Mexico. Final Report to Mississippi Department of Marine Resources and U.S. Fish and Wildlife Service, Award Number 067-C-Sargassum Study 135.

Garcia-Pineda, O., MacDonald, I., Hu, C., Svejkovsky, J., Hess, M., Dukhovskoy, D., Moorey, S., 2013. Detection of floating oil anomalies from the Deepwater Horizon oil spill with synthetic aperture radar. Oceanography 26 (2), 124–137. http://dx.doi.org/10.5670/oceanog.2013.38.

Gower, J., King, S., 2011. Distribution of floating *Sargassum* in the Gulf of Mexico and the Atlantic Ocean mapped using MERIS. Int. J. Remote Sens. 32, 1917–1929.

Gower, J., Hu, C., Borstad, G., King, S., 2006. Ocean color satellites show extensive lines of floating *Sargassum* in the Gulf of Mexico. Geosci. Remote Sens. IEEE Trans. 44, 3619–3625.

Gower, J., Young, E., King, S., 2013. Satellite images suggest a new *Sargassum* source region in 2011. Remote Sens. Lett. 4, 764–773.

Graettinger, G., Holmes, J., Garcia-Pineda, O., Hess, M., Hu, C., Leifer, I., MacDonald, I., Muller-Karger, F., Svejkovsky, J., 2015. Integrating data from multiple satellite sensors to estimate daily oiling in the northern Gulf of Mexico during the Deepwater Horizon oil spill. (FE_TR.31). DWH Natural Resource Exposure NRDA Technical Working Group Report.

Hu, C., 2009. A novel ocean color index to detect floating algae in the global oceans. Remote Sens. Environ. 113, 2118–2129.

Hu, C., Weisberg, R.H., Liu, Y., Zheng, L., Daly, K.L., English, D.C., Zhao, J., Vargo, G.A., 2011. Did the northeastern Gulf of Mexico become greener after the Deepwater Horizon oil spill? Geophys. Res. Lett. 38, L09601 (doi:09610.01029/02011GL047184).

Hu, C., Feng, L., Hardy, R.F., Hochberg, E.J., 2015. Spectral and spatial requirements of remote measurements of pelagic *Sargassum* macro algae. Remote Sens. Environ. 167, 229–246. http://dx.doi.org/10.1016/j.rse.2015.05.022.

Huffard, C.L., von Thun, S., Sherman, A.D., Sealey, K., Smith Jr., K.L., 2014. Pelagic *Sargassum* community change over a 40-year period: temporal and spatial variability. Mar. Biol. 161 (12), 2735–2751.

Lapointe, B.E., 1995. A comparison of nutrient-limited productivity in *Sargassum natans* from neritic vs. oceanic waters of the western North Atlantic Ocean. Limnol. Oceanogr. 40, 625–633.

Lapointe, B.E., West, L.E., Sutton, T.T., Hu, C., 2014. Ryther revisited: nutrient excretions by fishes enhance productivity of pelagic *Sargassum* in the western North Atlantic Ocean. J. Exp. Mar. Biol. Ecol. 458, 46–56.

MacDonald, I.R., Garcia Pineda, O.M., Beet, A., Daneshgar Asl, S., Feng, L., French McCay, D.P., Graettinger, G., Holmes, J., Hu, C., Leifer, I., Mueller-Karger, F., Solow, A.R., Swayze, G., 2015. Natural and unnatural oil slicks in the Gulf of Mexico. J. Geophys. Res. http://dx.doi.org/10.1002/2015JC011062.

Marmorino, G.O., Miller, W., Smith, G.B., Bowles, J.H., 2011. Airborne imagery of a disintegrating *Sargassum* drift line. Deep-Sea Res. I Oceanogr. Res. Pap. 58, 316–321.

McDonald, T.L., 2015. Calibration curves for Landsat derived *Sargassum* proportions. (WC_TR.25). DWH Water Column NRDA Technical Working Group Report.

McDonald, T.L., Powers, S.P., 2015. Estimates of *Sargassum* extent in four regions of the northern Gulf of Mexico from aerial surveys. NRDA Technical Report, p. 19.

McNutt, M., Camilli, R., Guthrie, G., Hsieh, P., Labson, V., Lehr, B., Maclay, D., Ratzel, A., Sogge, M., 2011. Assessment of flow rate estimates for the Deepwater Horizon/Macondo well oil spill. Flow Rate Technical Group Report to the National Incident Command, Interagency Solutions Group, March 10, p. 2011.

Milledge, J.J., Nielsen, B.V., Bailey, D., 2015. High-value products from macroalgae: the potential uses of the invasive brown seaweed, *Sargassum muticum*. Rev. Environ. Sci. Bio/Technol. 15, 67–88.

Powers, S.P., Hernandez, F.J., Condon, R.H., Drymon, J.M., Free, C.M., 2013. Novel pathways for injury from offshore oil spills: direct, sublethal and indirect effects of the Deepwater Horizon oil spill on pelagic *Sargassum* communities. PLoS One 8, e74802.

Rooker, J.R., Turner, J.P., Holt, S.A., 2006. Trophic ecology of *Sargassum*-associated fishes in the Gulf of Mexico determined from stable isotopes and fatty acids. Mar. Ecol. Prog. Ser. 313, 249–259.

Schell, J.M., Goodwin, D.S., Siuda, A.N.S., 2015. Recent *Sargassum* inundation events in the Caribbean: shipboard observations reveal dominance of a previously rare form. Oceanography 28 (3), 8–10.

South Atlantic Fishery Management Council, 2002. Fishery management plan for pelagic *Sargassum* habitat of the South Atlantic region. http://safmc.net/Library/pdf/SargFMP.pdf (228 pp.).

Sun, S., Hu, C., Feng, L., Swayze, G.A., Holmes, J., Graettinger, G., MacDonald, I.R., Garcia Pineda, O.M., Leifer, I., 2016. Oil slick morphology derived from AVIRIS measurements of the Deepwater Horizon oil spill: implications for spatial resolution requirements of remote sensors. Mar. Pollut. Bull. 103, 276–285. http://dx.doi.org/10.1016/j.marpolbul.2015.12.003.

United States of America v. BP Exploration & Production, Inc., et al., 2015n. Findings of fact and conclusions of law: phase two trial. Re: Oil Spill by the Oil Rig "Deepwater Horizon" in the Gulf of Mexico, on April 20, 2010, No. MDL 2179, 2015 WL 225421 (LA. E.D. Jan. 15, 2015). (Doc. 14021). U.S. District Court for the Eastern District of Louisiana Retrieved from http://www.laed.uscourts.gov/OilSpill/Orders/1152015FindingsPhaseTwo.pdf.

Witherington, B., Hirama, S., Hardy, R., 2012. Young sea turtles of the pelagic *Sargassum*-dominated drift community: habitat use, population density, and threats. Mar. Ecol. Prog. Ser. 463, 1–22.